Mem. S.A.It. Vol. 82, 658

Memorie della

The intra-cluster magnetic field power spectrum in Abell 2199

V. Vacca[1,2], M. Murgia[2], F. Govoni[2], L. Feretti[3], G. Giovannini[3,4], R. A. Perley[5], and G. B. Taylor[5,6]

[1] Dip. di Fisica, Univ. Cagliari, Cittadella Universitaria, I–09042 Monserrato (CA), Italy
[2] INAF - OAC, Poggio dei Pini, Strada 54, I–09012 Capoterra (CA), Italy
e-mail: vvacca@oa-cagliari.inaf.it
[3] INAF - IRA, Via Gobetti 101, I–40129 Bologna, Italy
[4] Dipartimento di Astronomia, Univ. Bologna, Via Ranzani 1, I–40127 Bologna, Italy
[5] Adjunct Astronomer at the NRAO, Socorro, NM 87801 USA
[6] Dep. of Physics and Astronomy, Univ. of New Mexico, Albuquerque NM, 87131, USA

Abstract. We investigate the magnetic field power spectrum in the cool core galaxy cluster A2199 by analyzing the polarized emission of the central radio source 3C 338. We use Very Large Array observations at 1.4, 5, and 8 GHz to produce detailed Faraday rotation measure and fractional polarization images of the radio galaxy. By comparing the observations and the predictions of 3D magnetic field models with a Bayesian approach, we constrain the strength and structure of the magnetic field associated with the intra-cluster medium.

Key words. Galaxies: cluster: general – Galaxies: cluster: individual: A2199 – Magnetic fields – Polarization – Cosmology: large-scale structure of Universe

1. Introduction

Linearly polarized radiation propagating through a magnetized plasma experiences a rotation of the plane of polarization which is proportional to the thermal gas density and the magnetic field strength along the line-of-sight. Indeed, it is possible to obtain important information about the intra-cluster magnetic fields by combining polarization images of radio sources located inside or behind galaxy clusters with X-ray observations of the thermal gas.

In this contribution, we investigate the magnetic field power spectrum in the nearby galaxy cluster A2199[1] by analyzing multi-frequency polarization observations of the central radio source 3C 338. A2199 is an interesting target for Faraday rotation studies because of the presence of X-ray cavities associated with the radio galaxy lobes (Johnstone et al. 2002), indicating that the rotation of the polarization plane is likely to occur entirely in the intra-cluster medium (ICM), since comparatively little thermal gas should be present inside the radio emitting plasma. A previous rotation measure (RM) study has been done by Ge & Owen (1994) based on 5 GHz Very Large Array (VLA) data. By combining the information from this RM image with de-

Send offprint requests to: V. Vacca

[1] z=0.0311 (Smith et al. 1997), 1″=0.61 kpc

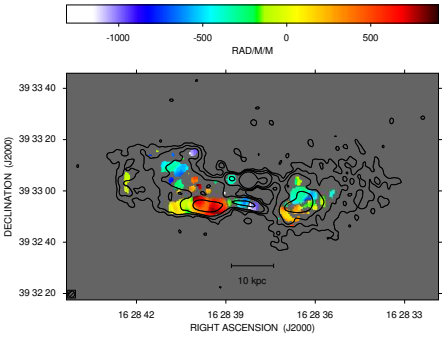

Fig. 1. Total intensity radio contours of 3C 338 at 8 GHz overlaid to the RM image of the radio galaxy 3C 338. The angular resolution is 2.5″×2.5″. Contour level are drawn at: 0.06, 0.12, 0.24, and 0.96 mJy/beam.

projected ROSAT data, and assuming a very simple magnetic field model, Eilek & Owen (2002) inferred an averaged magnetic field value along the line of sight of 15 μG.

In this work we try to improve upon the previous estimate by analyzing additional data and by performing a numerical modeling of the intra-cluster magnetic field fluctuations. Following Murgia et al. (2004), we simulate Gaussian random 3D magnetic field models with different power law power spectra and we compare the synthetic and the observed images in order to constrain the strength and structure of the magnetic field associated with the ICM.

2. Faraday rotation analysis

The presence of a magnetic field in an ionized plasma creates a difference in the phase velocities for left versus right circularly polarized radiation. As a consequence, the polarized emission from a radio source propagating through the plasma experiences a phase shift between the two components. This corresponds to a rotation in the polarization angle. For a completely foreground screen, as we expect here, the rotation is

$$\Psi_{\rm obs}(\lambda) = \Psi_{\rm int} + \lambda^2 {\rm RM}, \quad (1)$$

where $\Psi_{\rm obs}(\lambda)$ is the observed position angle at wavelength λ, and $\Psi_{\rm int}$ is the intrinsic polarization angle of the polarized emission. By considering an electron density $n_{\rm e}$, a magnetic field $\mathbf{B}$, and a path length $\mathbf{l}$, the Faraday RM is:

$${\rm RM} = 812 \int_0^{\rm l} n_{\rm e[cm^{-3}]} \mathbf{B}_{[\mu{\rm G}]} \cdot \mathbf{dl}_{\rm [kpc]} \quad {\rm rad\ m^{-2}} \quad (2)$$

We produced the Faraday RM image by running the FARADAY code (Murgia et al. 2004). The RM image is created by fitting pixel by pixel the observed polarization angle $\Psi_{\rm obs}$ versus the squared wavelength λ^2 (see Eq. 1) for all the frequencies.

The final RM image of 3C 338 is shown in Fig. 1 with total intensity contours at 8 GHz overlaid. The image has a resolution of 1.5 kpc. The RM has a patchy structure, and its distribution is characterized by a mean value of $\langle {\rm RM} \rangle$ =-54 rad/m^2 and a standard deviation $\sigma_{\rm RM}$ =460 rad/m^2. Unresolved RM structures in the foreground screen cause a progressive reduction of degree of polarization of the source (i.e. depolarization, see § 4), because of an incoherent sum of the radio signal.

3. Magnetic field modeling

We choose to model a power law power spectrum with index n of the form

$$|{\rm B}_k|^2 \propto k^{-{\rm n}} \quad (3)$$

in the wave number range from $k_{\rm min}$ to $k_{\rm max}$ and 0 outside. Moreover, we suppose that the power spectrum normalization varies with the distance from the cluster center such that the average magnetic field strength scales as a function of the thermal gas density according to

$$\langle {\rm B}(r) \rangle = \langle {\rm B}_0 \rangle \left[\frac{n_{\rm e}(r)}{n_0} \right]^{\eta} \quad (4)$$

where $\langle {\rm B}_0 \rangle$ is the average magnetic field strength at the center of the cluster and $n_{\rm e}(r)$ is the thermal electron gas density, taken from Johnstone et al. (2002).

Overall, our magnetic field model depends on five parameters: the strength at the cluster center $\langle {\rm B}_0 \rangle$, the radial slope η, the power spectrum index n, and finally the minimum and the maximum scale of fluctuation, $\Lambda_{\rm min} = 2\pi/k_{\rm max}$ and $\Lambda_{\rm max} = 2\pi/k_{\rm min}$, respectively.

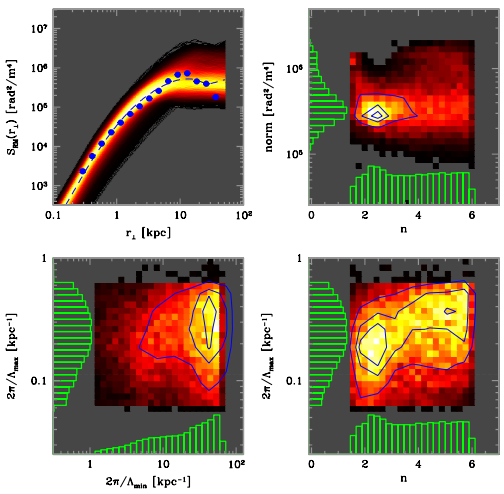

Fig. 2. *Top left panel*: Bayesian analysis of the RM structure function. The dots represent the data (error bars are comparable to the size of the symbols). The shaded area represents the population of synthetic RM structure functions from the posterior distribution. The dashed line corresponds to the most probable value for the model parameters. *Top right, and bottom panels*: 1-dimensional (histograms) and 2-dimensional (colors and contours) marginalization of the posterior for the model parameters. The contours are traced at 0.9, 0.75, and 0.5 the peak value.

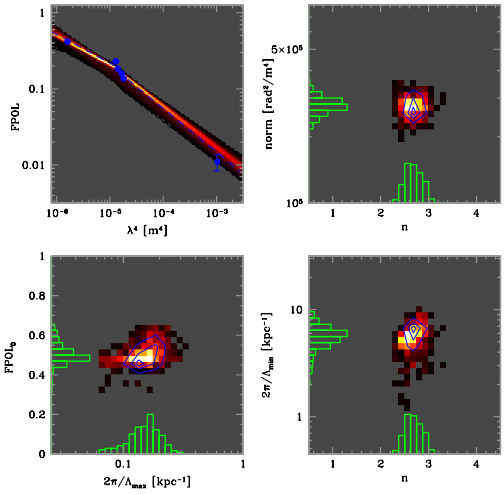

Fig. 3. *Top left panel*: Bayesian analysis of the source depolarization. The dots represent the data. The shaded area represents the population of synthetic polarization from the posterior distribution. The dashed line corresponds to the most probable value for the model parameters. *Top right, and bottom panels*: 1-dimensional (histograms) and 2-dimensional (colors and contours) marginalization of the posterior for the model parameters. The contours are traced at 0.9, 0.75, and 0.5 the peak value.

4. Results from 2D and 3D analysis

To constrain the magnetic field strength and structure, we proceeded in two steps. First, we performed a 2D analysis of the RM fluctuations and of the source depolarization to constrain the slope n and the range of scales of the power spectrum. Second, we performed 3D numerical simulations to constrain the strength of the field and its scaling with the gas density. In both cases, we made use of the FARADAY code to produce synthetic polarization images of 3C 338 and to compare them to the observed ones by means of the Bayesian inference, whose use has been first introduced in the RM analysis by Enßlin & Vogt (2003). The synthetic images are gridded to the same geometry as the data and are convolved to the same angular resolution. Moreover, we masked the synthetic images using the observations in order to reproduce the window function imposed by the shape of 3C 338, and we added Gaussian noise, in order to mimic the noise of the observed RM image.

In particular, we characterize the RM image by its structure function $S_{\rm RM}(r_\perp)$, which is obtained by averaging RM values corresponding to pixels located at the scale distance $r_\perp$. We then applied the Bayesian method by choosing uniform priors for the four free power spectrum parameters: the normalization *norm*, the minimum and the maximum scale of fluctuation $\Lambda_{\rm min}$, and $\Lambda_{\rm max}$, and the slope n. In Fig. 2 we show the results of the Bayesian analysis of the RM structure function. The maximum scale of fluctuation, the normalization, and the slope of the power spectrum appear to be characterized by a peak that corresponds to the maximum posterior probability for that configuration of parameters, while for the minimum scale of fluctuation we have just an upper limit.

The power spectrum used to model the RM image should also be consistent with the observed depolarization of the radio source at in-

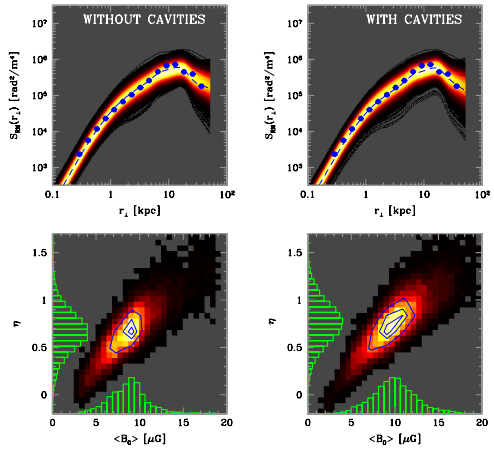

Fig. 4. Bayesian 3D analysis of the RM structure function for the model with (right) and without (left) cavities. *Top panels*: The dots represent the data (error bars are comparable to the size of the symbols). The shaded area represents the population of synthetic RM structure functions from the posterior distribution. The dashed line corresponds to the most probable value for the model parameters. *Bottom panels*: 1-dimensional (histograms) and 2-dimensional (colors and contours) marginalization of the posterior for the model parameters. The contours are traced at 0.9, 0.75, and 0.5 the peak value.

creasing wavelengths. In Fig. 3 the posterior from the depolarization analysis is shown for the five free parameters: the intrinsic degree of polarization $FPOL_0$, the normalization *norm*, the slope n, the minimum, and the maximum scale of fluctuation $\Lambda_{\rm min}$, and $\Lambda_{\rm max}$ of the magnetic field power spectrum. All the model parameters appear to be well constrained, and their values are consistent with the structure function analysis.

Overall, the combined 2D analysis, RM image and depolarization, allowed us to constrain the power spectrum index to n=(2.8±1.3), and the minimum and maximum scale on the range from $\Lambda_{\rm min}$ =(0.7±0.1) kpc to $\Lambda_{\rm max}$ = (35±28) kpc. In the next step we fix these values and we constrain the strength of the magnetic field and its scaling with the gas density with the aid of 3D simulations.

The result of the Bayesian analysis for 3D magnetic field models is shown in Fig. 4 (left panels) for the two free parameters: the strength at the cluster center $\langle B_0 \rangle$, and the radial slope η. The two parameters appear well constrained. We found a magnetic field with a central strength $\langle B_0 \rangle$=(9.6±2.3) μG, and a radial slope η=(0.7±0.2).

Hence, we tried to improve our analysis by including the X-ray cavities in the 3D modeling. In particular, we removed from the 3D simulations the gas density inside two ellipsoidal regions centered on the radio lobes. We repeated the Bayesian analysis including the cavity information and we found $\langle B_0 \rangle$=(10.1±2.6)μG, and η=(0.8±0.2) (see Fig. 4, right panels).

Acknowledgements. This work makes use of results produced by the Cybersar Project managed by the Consorzio COSMOLAB, a project co-funded by the Italian Ministry of University and Research (MIUR) within the Programma Operativo Nazionale 2000-2006 "Ricerca Scientifica, Sviluppo Tecnologico, Alta Formazione" per le Regioni Italiane dell'Obiettivo 1 (Campania, Calabria, Puglia, Basilicata, Sicilia, Sardegna) Asse II, Misura II.2 "Societá dell'Informazione", Azione a "Sistemi di calcolo e simulazione ad alte prestazioni". More information is available at http://www.cybersar.it. This research was partially supported by ASI-INAF I/088/06/0 - High Energy Astrophysics and PRIN-INAF2005. The National Radio Astronomy Observatory (NRAO) is a facility of the National Science Foundation, operated under cooperative agreement by Associated Universities, Inc. We are grateful to Antonella Fara and Riccardo Pittau for the assistance with the Cybersar-OAC computer cluster.

References

Enßlin, T. A., & Vogt, C. 2003, A&A, 401, 835
Eilek, J. A., & Owen, F. N. 2002, ApJ, 567, 202
Ge, J., & Owen, F. N. 1994, AJ, 108, 1523
Johnstone, R. M., et al. 2002, MNRAS, 336, 299
Murgia, M., et al. 2004, A&A, 424, 429
Smith, R. J., et al. 1997, MNRAS, 291, 461